Results in Materials 6 (2020) 100091

Contents lists available at ScienceDirect

Results in Materials

journal homepage: www.journals.elsevier.com/results-in-materials

In vitro evaluation of poly-ε-caprolactone-hydroxypatite-alumina electrospun fibers on the fibroblast's proliferation

Ana Karen Monrreal-Rodríguez, Jesús Alberto Garibay-Alvarado, Claudia Lucía Vargas-Requena, Simón Yobanny Reyes-López *

Instituto de Ciencias Biomédicas, Universidad Autónoma de Ciudad Juárez, Envolvente Del PRONAF y Estocolmo S/n, Ciudad Juárez, Chih, C.P. 2300, Mexico

ARTICLE INFO

Keywords:
Cell viability
Poly ε-caprolactone
Hydroxyapatite
Alumina

ABSTRACT

A biomaterial can replace the function of a real organ, conferring properties of support, regeneration or resistance. In the present investigation, a new composite was developed in the form of a polymeric membrane embedded with hydroxyapatite and alumina particles to be used as scaffolding and to allow cell viability. The support matrix is poly ε-caprolactone, which is a biodegradable polymer, hydroxyapatite is the ceramic that contributes to the improvement of osteoconductive and osteo-regenerative properties, while alumina provides the hardness to the composite for its viable application in the orthopedic industry. The morphology of the composite resulted in an interweaving of fibers with a diameter of 840 ± 230 nm. The composites were analyzed to the MTT cytotoxicity test, showing that none of the composites were toxic ($p = 0.0001$); where the PCL/HA/α-Al_2O_3 composite showed greater cellular viability with 238%, demonstrating its possible usefulness as orthopedic material, in filling fractures, or bone imperfections caused by physical damage.

1. Introduction

The orthopedic, dental and biomedical area seeks to develop materials with compatibility qualities in the human body to increase the quality of life in patients who have suffered bone loss or damage. The developed materials must have the capacity to fill and support the loading efforts to which they are exposed, as well as being biochemically compatible. Synthetic hydroxyapatite (HA) is a compound with biomedical applications, due to its similarity to the inorganic phase of human bone [1–3]. HA based materials are bioactive and tend to be porous, allowing bone ingrowth and can also be absorbed into the organism [4]. HA can be used for dental or orthopedic applications, alone, and in conjunction with autologous and allogeneic bone grafts, or in composites as bone cement for the repair of facial skull defects, or as graft material for the repair of the bone defects [5]. However, hydroxyapatite has great fragility, which is why its mechanical stability limits its use for the regeneration of bone defects [2,3,5].

Most of the composite materials used in the orthopedic and dental areas must have regenerative, biocompatibility and resistance properties and any new material designed for this purpose has to achieve some or all of these characteristics [6–15]. Poly ε-caprolactone (PCL) is a biocompatible and biodegradable polymer [6,20,22], and that in combination with other materials has shown regenerative characteristics, allowing cell adhesion [7,8]. α-alumina (α-Al_2O_3) has been extensively used in orthopedic and dental applications because of its great resistance and chemical inertia, Sopyan et al. [4,11,22] have shown that the addition of Al_2O_3 together with HA increases the resistance to compression, without being toxic and allowing the adhesion of osteoblasts [9]. The use of PCL fibers with HA and α-Al_2O_3 particles is proposed, where PCL is used as biodegradable material, which serves as a transport of HA and α-Al_2O_3 particles, obtaining a resistant, biodegradable and regenerative material. The addition of HA allows for improvements in the osteoconductive and osseointegration properties, as reported by Malik et al. [9], shown to help better adhesion and facilitates cell growth [3,10]. The aim of this project was to a develop a composite in the form of a polymer membrane embedded with hydroxyapatite-alumina particles that act as scaffolding and allow cell viability.

2. Materials and methods

2.1. Synthesis hydroxyapatite nanopowders

Hydroxyapatite was prepared using the precipitation method, whereby $Ca(NO_3)_2.4H_2O$ (ACS, Sigma-Aldrich©) and $(NH_4)_2HPO_4$ (ACS,

* Corresponding author.
E-mail address: simon.reyes@uacj.mx (S.Y. Reyes-López).

https://doi.org/10.1016/j.rinma.2020.100091
Received in revised form 10 February 2020; Accepted 29 February 2020
Available online 2 April 2020

Table 1
Parameters for obtaining fibers by the electrospinning method.

Parameters/ Compound	Distance (cm)	Humidity (%)	Voltage (Kv)	Flow rate (µl/ min)	Diameter (µm)
PCL	10	40	8	15	0,84 ± 0,23
PCL-HA	12	35	11	10	0.96 ± 0.32
PCL- α-Al_2O_3	12	39	9	13	1.13 ± 0.41
PCL-HA- α-Al_2O_3	13.5	42	11	16	1.39 ± 0.64

Alfa Aesar©) were dissolved in deionized water separately. The Phosphate solution was then added dropwise into the nitrate solution and mixed under constant magnetic stirring for 60 min. The pH of the final solution was adjusted to 11 using NH_4OH (Jalmek©) and stirred for additional 60 min at ambient temperature. The formed precipitate was separated from the liquid by centrifuging at 12,500 rpm and washed twice with deionized water and once with isopropanol centrifuging between each wash. The precipitate was thermally treated in a high temperature oven (Thermo scientific© Heratherm™) at 100 °C for 24 h and then in a crucible (Thermo scientific© Thermoline™) at 800 °C for 2 h with a heating ramp of 5 °C/min.

2.2. Synthesis alumina nanopowders

For the synthesis of alpha alumina nanoparticles, emulsions were prepared from metalorganic precursor aluminum formate and urea, using ethanol as solvent, until obtaining a homogeneous white paste. Aluminum formate $Al(O_2CH)_3$ was obtained by chemical synthesis described by Reyes et al. [11] involving a mixture of aluminum with formic acid (HCOOH) using mercuric chloride ($HgCl_2$) as catalyst to obtain the aluminum formate solution which was spray dried to produce fine granulated metal-organic precursor. Heat treatment was done by microwave combustion; each of the emulsions was exposed to microwaves (1000 w) for 5 min to obtain porous agglomerates. The agglomerates were calcined in a muffle furnace at a temperature of 1050 °C for 1 h in an oxygen rich atmosphere, using a 10 °C/min curve. After calcination, the fragile agglomerates were ground in an agate mortar to obtain fine alumina powders.

2.3. Preparation of solutions for fibrillar membranes

For the elaboration of the solutions, poly ε-caprolactone (PCL) (ACS, Sigma-Aldrich©) was diluted in acetone at 10%, later were added 2% of HA powder, 2% of α-Al_2O_3 powder, and also a solution of PCL, HA and α-Al_2O_3 was prepared, keeping them in magnetic agitation for 1 h and in ultrasonic bath for 1 h. The precursor solutions were transferred to 10 mL glass syringes (Fortuna© Optima™) and placed in an injection pump (KD© Scientific™). The distance to the collector of 10–14 cm was used during electrospinning process, feeding rate was 10–16 µl/min, while voltage was 8–11 kV. Fibers were collected on a rotating drum covered with aluminum foil. Environmental parameters during electrospinning process were 21 °C and 35–42% for Temperature and Relative Humidity, respectively. Four different fibrillar composites were made: PCL, PCL-HA, PCL-α-Al_2O_3 and PCL-HA-α-Al_2O_3.

Characterization of as-spun fibers was carried out by Fourier Transformed Infrared Spectroscopy with a Bruker© Alpha Platinum™ ATR instrument by Attenuated Total Reflection technique, with 40 scans and resolution of 4 cm^{-1}. Morphology and diameters were determined by Scanning Electron Microscopy with an instrument JEOL© JSM-6010 PLUS/LA™. Thermogravimetric analysis (TGA), Differential vcsamples were also characterized by Raman spectroscopy using a 532 nm laser scanning an area of 5 µm, and crystalline phases were identified by XRD with a PANalytical© X'Pert™ PRO diffractometer (Cu Kα1, 35 kV, 25 mA) with scanning range from 20 to 80° and 2°/min scan speed.

2.4. In situ assay

2.4.1. Cell culture

The Primary Dermal Fibroblast Normal Human, Neonatal (HDFn) was obtained from ATCC® (PCS-201-010™) and were cultured in Dulbecco's modified Eagle's medium (DMEM, SIGMA, D5523) with supplements of 10% fetal bovine serum (FBS) and 1% penicillin/streptomycin, at 37 °C in a humidified atmosphere with 5% CO2 and 95% air (SHELLAB, SL2406). The culture medium of both was refreshed every two days; upon confluence, cells were rinsed with 2 mL of phosphate buffered saline (PBS) solution and incubated with 5 mL of 0.05% trypsin-EDTA at 37 °C in a humidified atmosphere with 5% CO2. Next, within 1–2 min, the trypsin enzyme activity was stopped by the addition of 5 mL of complete growth medium and centrifuged for 5 min at 3000 rpm. The supernatant was discarded, while the cells were suspended in fresh medium and seeded onto culture flasks for further propagation and subsequent passages. Cells from 2nd to 4th passages were seeded on composites to measure its growth.

2.4.2. Cell viability

The PCL nanofibers were cut into round pieces (5.5 mm in diameter) and disinfected by exposure to UV light for 30 min on each side, were

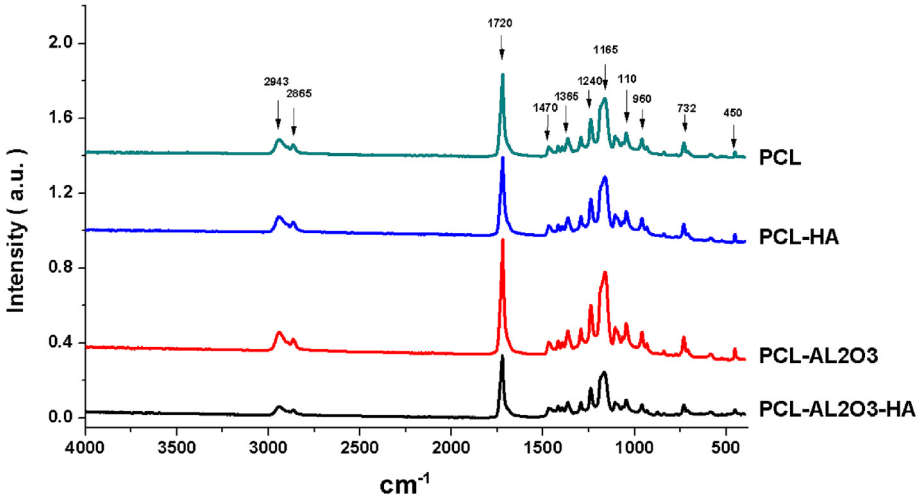

Fig. 1. Identification of functional groups present in the polymer membranes. Poly ε-caprolactone (PCL), Hydroxyapatite (HA), Alumina (α-Al_2O_3).

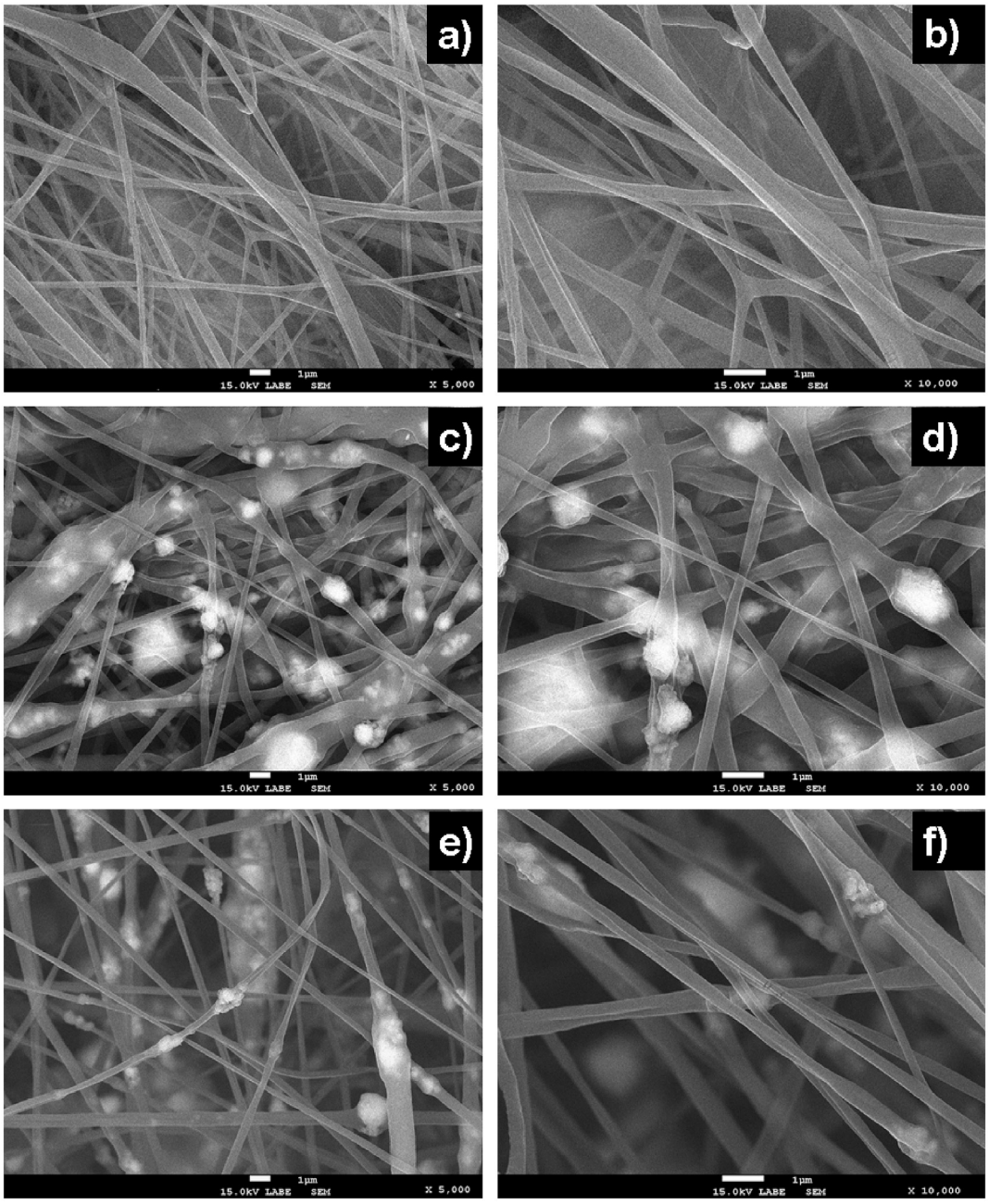

Fig. 2. Morphology of the PCL fibers at 5,000× (a) and 10,000× (b); PCL-HA fibers at 5,000× (c) and 10,000× (d); and PCL-α-Al_2O_3 fibers at 5,000× (e) and 10,000× (f).

then placed in a 96-well plate and seeded with 5000 cells per well; tissue culture plate was used as control. Cell viability was measured at time points of 24, 48 and 72 h using MTT reagent (3–4,5-dimethylthiazol-2-yl) −2,5-diphenyltetrazolium bromide, Sigma-Aldrich©), 0.5 mg/mL in PBS (Tran et al., 2015). On the day of measurement, medium was carefully replaced on fresh DMEM +10% FBS with diluted MTT (1:10, 10% MTT), and incubated for 1 h at 37 °C in a CO2 incubator to allow the transformation of MTT dye to formazan salt. After removing incubation medium, formazan crystals were dissolved in 100 μl solution of DMSO. MTT reduction was quantified by measuring the light absorbance at 570 nm using the Benchmark Plus absorbance microplate reader (BioRad©). MTT test was repeated nine times. Percentage of viability was calculated by the following formulation:

$$Viability\ (\%) = \frac{OD\ Treated\ cells}{OD\ Control\ cells} X100$$

3. Results and discussion

3.1. Composites fabrication

The PCL composite used a distance of 10 cm and a flow of 15 μL/min, unlike the PCL-HA composite that used a distance of 12 cm, with a voltage of 11 Kv and a flow of 10 μL/min the difference flow is given by the change of humidity; in the PCL-α-Al_2O_3 fibers the distance was maintained at 12 cm, the voltage decreased to 9 Kv and the flow increased to 13 μL/min, due to conductivity of the alumina suspension. While for the fibers of PCL-HA-α-$A_{l2}O_3$ it was necessary to modify the

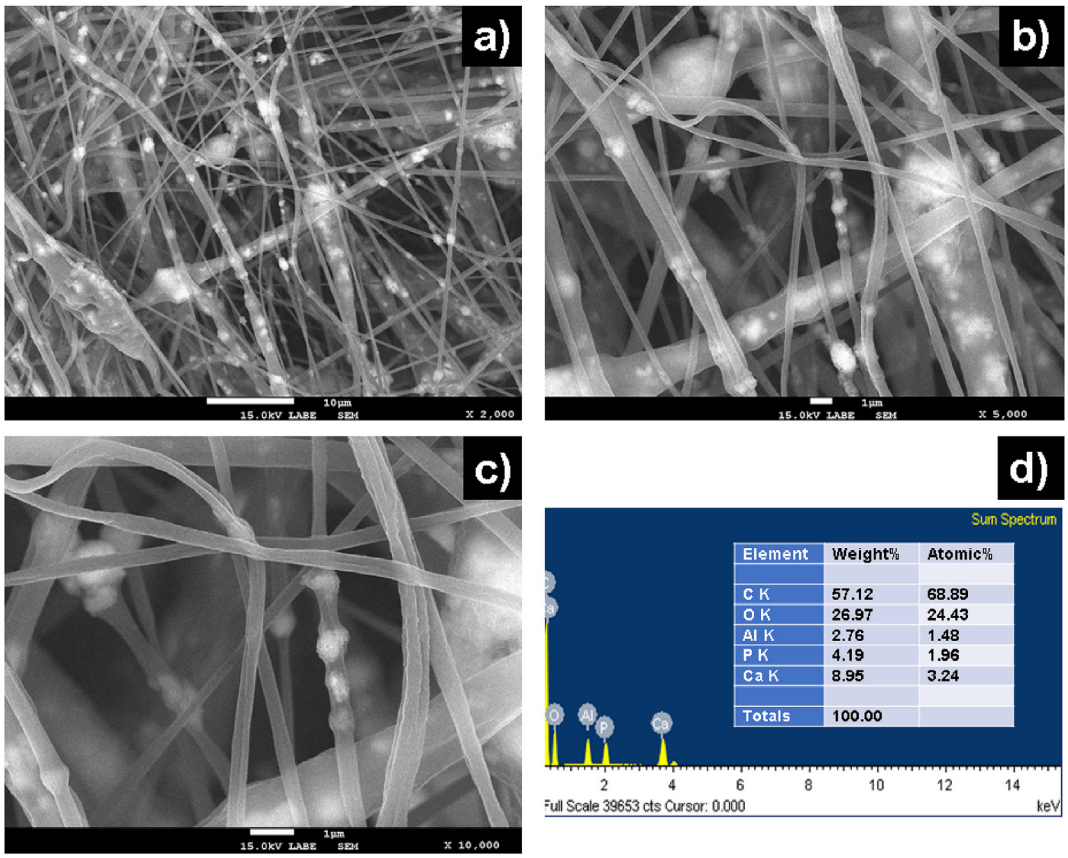

Fig. 3. Morphology of the PCL-HA-Al_2O_3 fibers observed at a) 2000×, b) 5000×, c) 10000× and the chemical composition in d) (EDX).

flow rate for the expulsion of the solution to the decrease of mobility presented by the increase of the ceramic used, the increase in voltage causes the expulsion of the particles when loading them helping the flow of the polymer which is affected by the humidity due to the hydrophobic characteristics presented by the polymer, hindering the evaporation of the solvent and the flow of this, the increase of the distance is due to the fact that a greater volatilization of the solvent and the lengthening of the fibers, The parameters used in the fabrication of the fibers is shown in Table 1.

3.1.1. FTIR analysis

Infrared spectroscopy was used to reaffirm the composition of the membranes and the presence of the ceramic particles that were suspended in the polymer solution. The infrared bands of the fibers have the same wavelengths, this is due to the fact that alumina and hydroxyapatite particles are found in a lesser proportion in the polymer suspension, in addition to being embedded in the polymer, infrared radiation does not penetrate the material, and it is not possible to observe

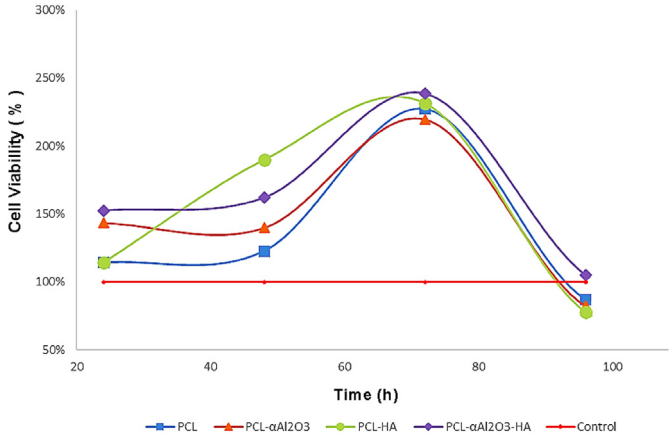

Fig. 4. Cellular proliferation on PCL, PCL-HA, PCL-α-Al_2O_3 and PCL-HA-α-Al_2O_3.

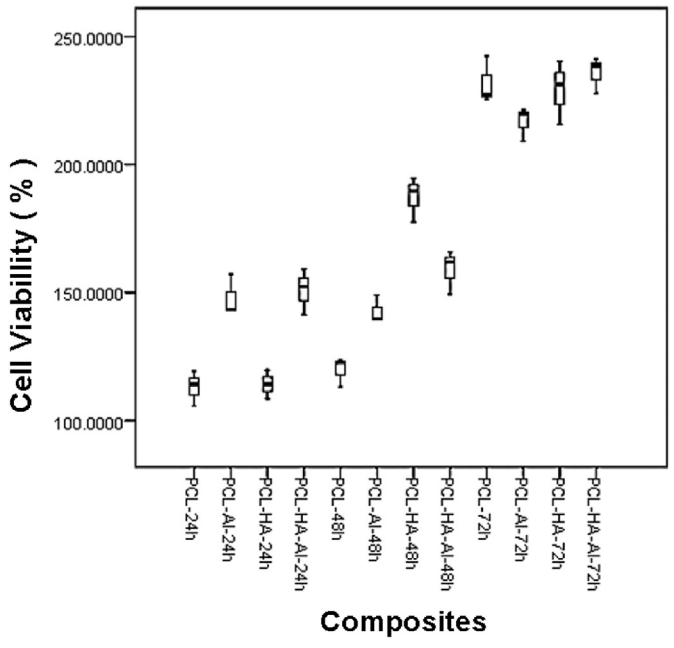

Fig. 5. Cellular growth comparison at different times from 24 to 120 h (*in the same group).

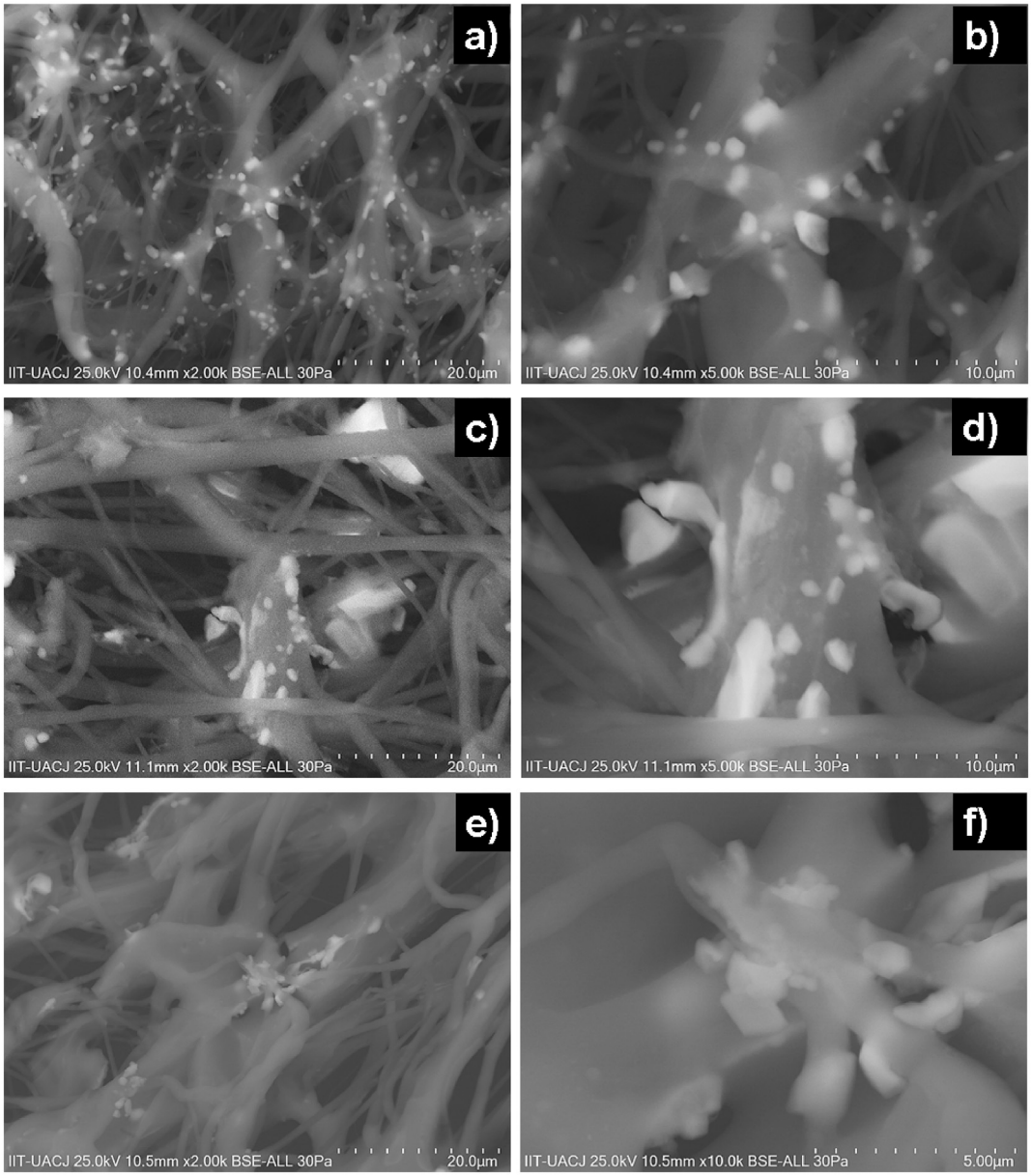

Fig. 6. Morphology of mineralization of the PCL fibers at 2,000× (a) and 5,000× (b); PCL-HA fibers at 2,000× (c) and 5,000× (d); and PCL-α-Al_2O_3 fibers at 2,000× (e) and 5,000× (f).

the characteristic vibrations of alumina and hydroxyapatite, obtaining only the characteristic vibrational bands of PCL. In the infrared spectrum of poly ε-caprolactone in Fig. 1, vibrations of asymmetric stretching at 2943 cm^{-1} for the CH_3 group and stretches by deformation at 2865 cm^{-1} for the methylene group, bands of vibrations by stretching to 1720 cm^{-1} for C═O, bands by crystalline stretching at 1365 and 1470 cm^{-1} for the COC group, and vibration bands by asymmetric stretching at 1240, 1110, 1165, 960, 732 and 450 cm^{-1} for the COC group. Vibrations were found at 2800 and 2650 cm^{-1} corresponding to $–CH_2$ [20,21,22].

In the DSC made of PCL an exothermic peak is observed at 62.35 °C, while in PCL-HA it increases to 62.38 °C and with PCL-αAl_2O_3 it increases to 62.72 °C, observing that when the ceramics are introduced, the melting point increases, showing that the PCL-α-Al_2O_3 fibers are the ones that need a greater application of heat to reach it's melting point, while in the crystallization process occurs at a lower temperature in the PCL fibers. The presence of ceramics diminishes the purity of the material causing the decrease of the energy needed to bring it to a point of fusion and crystallization of the material. It is important to know if the material can resist the temperatures present in the human body, high temperatures should not affect the material because the maximum temperature that can be reached by the human body is 41–42 °C.

3.1.2. SEM of the fibers before biological assays

In this work electrospinning technique was used because of its simplicity and effectiveness in making nanofibers. Additionally, in this method, fiber diameter was controlled to produce a scaffold of PCL, PCL-HA, PCL- α-Al_2O_3 and PCL-HA-α-Al_2O_3. Fig. 2 shows a sample of nanofibers of 10% PCL (2-a, 2-b), 10% PCL with 2% HA (2-c, 2-d) and 10% PCL with 2% α-Al_2O_3 (2-e, 2-f). It was observed that the fibers obtained from PCL, PCL and ceramics are unidirectional, with different diameters. Voltage controlled fibers formation, since it elongates and breaks surface tension of polymer solution. Increasing ceramic concentration caused instability of Taylor cone and an increase in fibers whipping movement.

SEM micrographs in Fig. 2-a and b shows the morphology of PCL fibers. The structure of fibers presents a random arrangement. The images show fibers with a cylindrical smooth surface, and are free of beads,

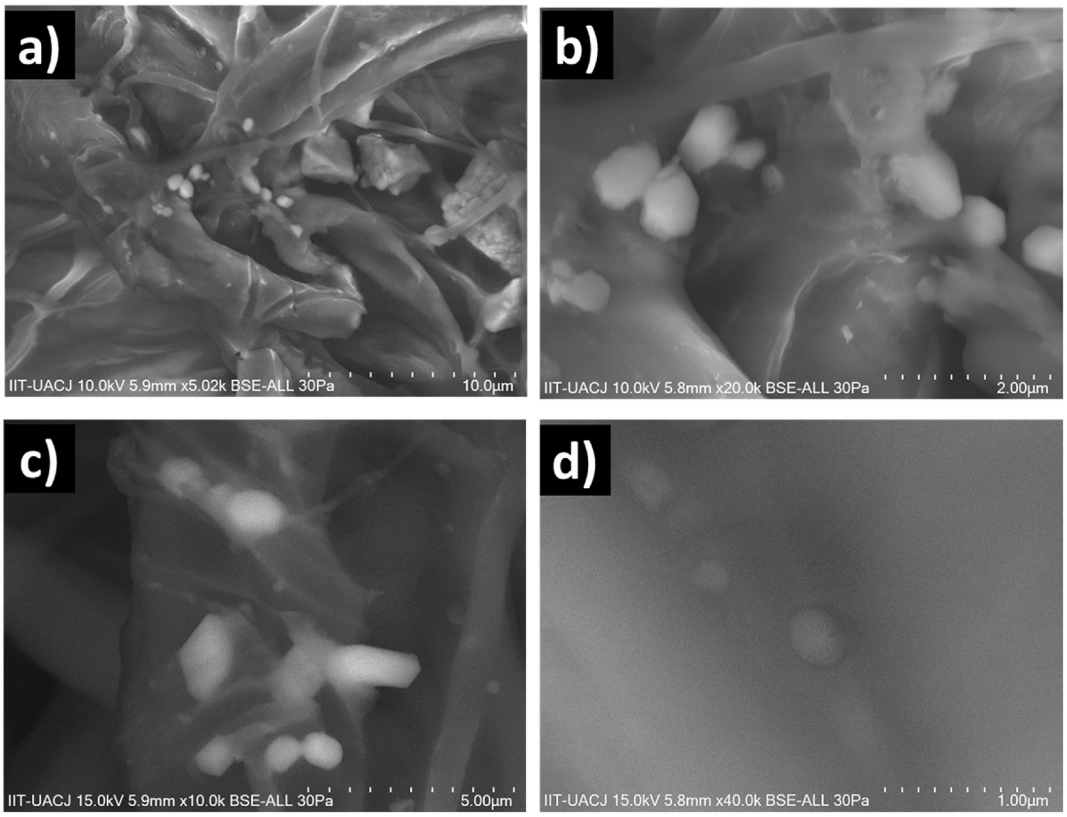

Fig. 7. Cells and mineralization over PCL-HA-α-Al_2O_3 fibers, at a) 5000×, b) 20000×, c) 10,000 × y d) 40,000 ×.

precipitates and fractures with a diameter of 0,84 ± 0,23 µm. Fig. 2-c and d shows the morphology of PCL-HA fibers. Fig. 2-d is a magnification of the sample were its observed that the HA is embedded in the PCL reaffirming the presence of HA dispersed in the polymer solution, it was also seen that the fiber is smooth and tubular, with a fibrillar size of 0.96 ± 0.32 µm. Fig. 2-e and f shows a sample of nanofibers of 10% PCL with 2% α-Al_2O_3. Fig. 2-e gives an overview of the fibers, where there are very few defects, allowing to observe a spindle shape, and that increase the average diameter of the fibers. In Fig. 2-f it's a magnification of the fibers, the α-Al_2O_3 particles are found in embedded in the upper part of the fiber in greater detail. It is possible to observe that the fibers are rough and continuous, however, they are distributed randomly along the plane and their diameter is variable. The fibers have an average size of 1.13 ± 0.41 µm. In addition, there are some agglomerations of α-Al_2O_3 in the external part of the fibers. The deformations were due to impact and angle on incidence of polymer jet on the collector, and thus obtaining polydisperse fibers and some agglomerations.

Fig. 3 shows the morphology of the nanofibers of PCL-HA-α-Al_2O_3 in different magnifications showing contrast between the particles of HA and α-Al_2O_3 presenting the particles of HA with a characteristic brightness, while the particles of α-Al_2O_3 look opaque. The fibers have a size of 1.39 ± 0.64 µm. The chemical composition of the fibers was obtained using the X-ray dispersive energy spectrometry (EDX) technique (Fig. 3d), showing carbon as the predominant element (57.12%) followed by oxygen (26.97%), then calcium (8.95%), phosphorus (4.19%) and aluminum (2.76%). Carbon is the predominant element because of the presence of poly ε-caprolactone, the presence of calcium, phosphorus, indicates the presence of hydroxyapatite present and aluminum the presence of alumina, oxygen is shown in said percentage since this is part of the three components.

Electrospun fibers tend to break and generate deformations at longer distances, while at short distances solvent do not volatilize at enough rates and generates agglomerations. It is observed that there is no great difference in the parameters used for the realization of fibers, but it can be seen that the small differences are visible in the size of the fibers, one of the parameters that influence is the flow in the fibers of PCL-HA-α-Al_2O_3, which is higher, causing an increase in the size of the fibers, unlike those of PCL-HA and PCL-α- Al_2O_3 that have a lower flow; while the size difference in the PCL-HA and PCL-α- Al_2O_3 fibers is due to the electrical conductivity causing the PCL-α- Al_2O_3 fibers to have a larger size because it has a higher electrical conductivity which facilitates greater output of the solution causing a greater size of the fibers. Thus, reduction in voltage, feeding rate, and decrease in ceramics nanoparticles concentration resulted in smaller diameters. The effect of crystallinity on biomaterials properties is important in the tissue engineering. The cell adhesion and proliferation are more in amorphous polymers.

3.1.3. *Cytotoxicity of composites*

Fig. 4 shows the results from the cell viability test carried out on the four membranes; finding out that the 4 of them are biocompatible and favor the cellular proliferation. In the case of the PCL-only membranes the viability values are 14, 22 and 127%, above than those of the control cells, at 24, 48 and 72 h of incubation, respectively. Its acceptance is due to the use of the polymer as an energy source; the PCL begins an oxidation process for the formation of lactic acid that is assimilated to transform into energy, helping in cell growth [13]. The PCL-HA membranes present increments of 14, 89 and 131% at the three incubation times, respectively; this acceptance could be related to the HA and its capacity for cellular conduction and induction; by providing the compound Ca^{2+} ions, which help on the suspension of HPO_4^{2-} allowing the assimilation of ions, establishing these chemical exchanges allows the formation of interfacial bonds in living tissue, favoring the integration process and tissue formation [14]. Obtaining pure HA allows us to have a composite which presents ions that provide the capacity of partial or complete replacement of PO_4^{3-} ions by HPO_4^{2-}, Ca^{2+} by K^+ or Mg^{2+}, and OH^- by F^-, Cl^-, Br^-, helping in the solubility and as a source of ions which will intervene in

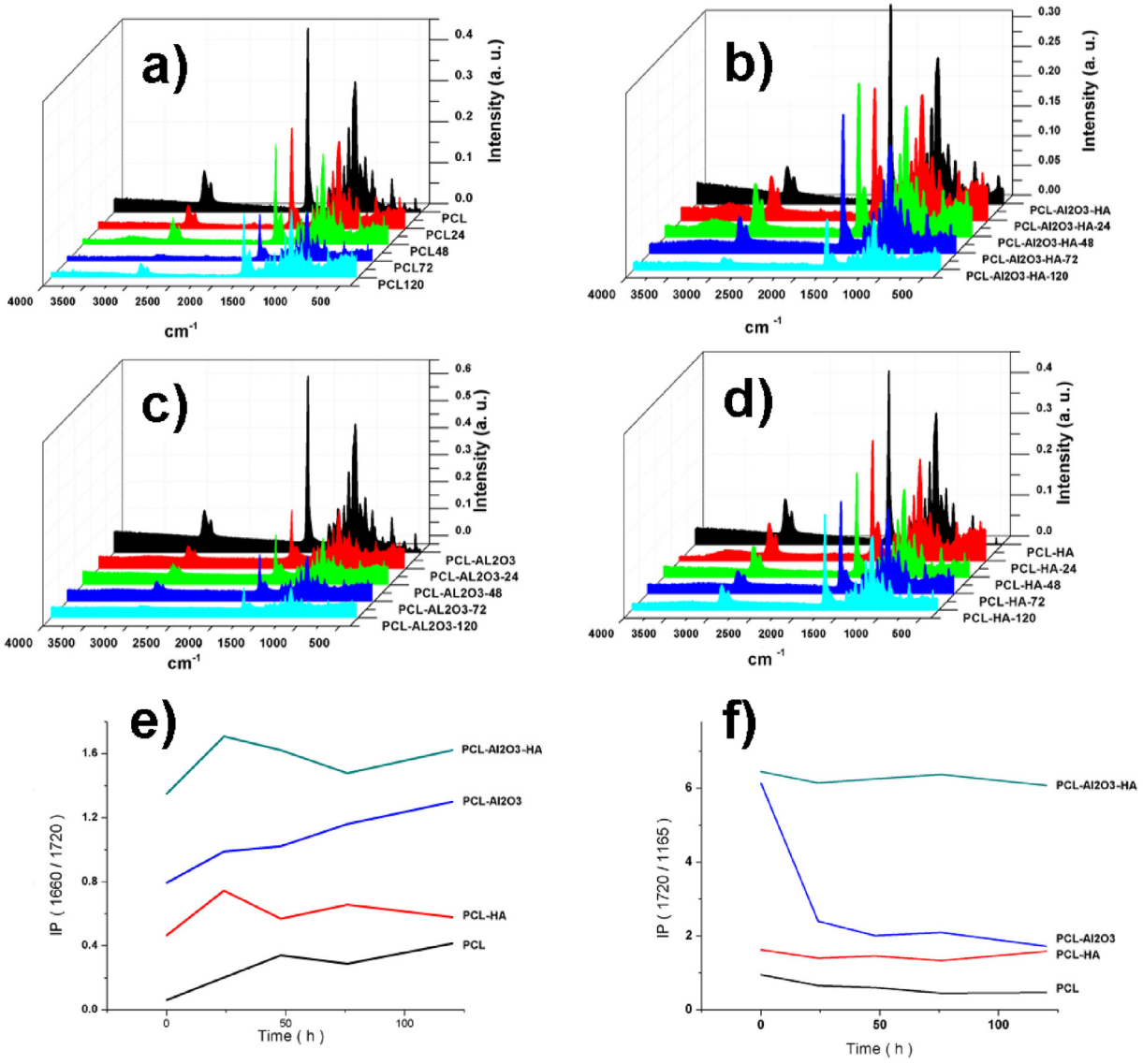

Fig. 8. IR spectra of cellular proliferation on a) PCL, b) PCL-HA, c) PCL-α-Al_2O_3, d) PCL-HA-α-Al_2O_3, e) $IP_{1660/1720}$ and f) $IP_{1720/1165}$.

the cellular metabolization helping the integration of the composite [18]. Moreover, the membranes embedded with α-Al_2O_3 particles present an increment of 43, 39 and 119% on cell growth at the three times of incubation with respect to the control; this increment is due to the fact that the alumina particles give greater firmness to the PCL polymer membrane, facilitation cellular mobility. Meanwhile the viability on the PCL-HA-α-Al_2O_3 reached values of 52, 61 and 138%, higher than those of the control at 24, 48 and 72 h of incubation.

In the data analysis (ANOVA) with a significance of 0.0001, as shown in Fig. 5 by means of a chart of boxes, the deviations presented in the study are ± 5, F = 240.61, 19° of freedom between groups, and 40° of freedom within the groups. In the analysis of comparisons by Tukey, there was no difference in growth at 72 h in the PCL-HA-α-Al_2O_3, PCL-HA and PCL composites, presenting greater proliferation, while the PCL-α-Al_2O_3 composite had a different level of cell growth, in addition it is observed that the same levels of viability were present in each incubation time, each one being different.

3.1.4. SEM of the fibers after biological assays

Fig. 6-a and b shows the fibers of PCL 48 h after the seeding of the cells; it is possible that when the fibroblasts were in contact with the material a mineralization process began, with forming of calcification sites of different shapes and sizes; the formation of calcifications can occur in a cell nest in the process of degeneration (cell death process) [15]. When the cells degenerate, calcium phosphate crystals can be deposited inside the cell, the mitochondria could be the first organelle to go through this process, because of the increased permeability of the membranes, therefore, the degenerating cell may serve as a nest for the calcification of a tissue [16]. It is possible that when comparing with the toxicity test the decrease in cell proliferation coincides with this phenomenon. The composite of PCL-HA when in contact with fibroblast cells results in a mineralization process, as seen in Fig. 6-c and d. The formation of crystals and the presence of vesicles contribute to the mineralization process. Hydroxyapatite is adsorbed and forms crystals in the form of needles on the inner surface of the membrane [16]. The composite of PCL-α-Al_2O_3 in contact with the fibroblast cells began a process of mineralization as well. In Fig. 6-e and f, the mineralization can be observed and through it, certain nodules which have different morphologies produced by the cells. Being the α-alumina a ceramic that allows the adhesion, proliferation and mineralization process [17]. The process of mineralization occurs when the vesicles create a specific environment for the deposition of minerals, allowing the formation of

crystals on the inner surface of the cell membrane and be released from the cell matrix. Crystals work as templates for the formation of crystalline matrices, which will lead tissue calcification of the tissue [18]. The production of crystals or nodules is lower because the alumina does not present chemical interaction directly with the cells, since alumina is inert and does not allow the complete adsorption of the composite, avoiding the multi-formation of crystals when not absorbed, showing crystals in smaller quantity unlike the PCL composite. The alumina does not present free radicals and the obtaining of the alpha phase allows to have a ceramic that has great stability characteristics unlike the other phases of alumina. It is possible the formation of stable mononuclear complexes with phosphate, fluoride, sulfates and silicate with alumina, competing with hydrolysis reactions in phosphate solutions, but also causing little interaction with the cells present in the medium, attributing lower cell viability.

The composite of PCL-HA-α-Al_2O_3 in Fig. 7 shows that not only favors cell adhesion and proliferation, but also allows mineralization, forming larger crystals in contrast to those present in the PCL-α-Al_2O_3 composite. Alumina is negatively charged at a physiological pH [19], a factor which may aid in the attraction of Ca^{2+} ions, facilitating the adhesion of the crystals formed by the cells. Ca^{2+} has an influence over the vesicles, promoting the activity of the ion channels forming collagen. In Fig. 7-c, collagen fibers can be observed entangled in the fibers of the composite. Collagen fibers could have an influence over the start and development of mineral formation [18].

3.1.5. FTIR analysis of the fibers after biological assays

Infrared spectroscopy was used to confirm the decomposition of the membranes and check the presence of the hydroxyapatite particles and collagen in to composite. In the infrared spectrum of composite in Fig. 8, vibrations of asymmetric stretching at 2943 cm^{-1} and stretches by deformation at 2865 cm^{-1} for the CH_3 decrease with the time of cellular growth from 0 to 120 h. Bands of vibrations at 1720 cm^{-1} for C═O, 1365 and 1470 cm^{-1} for the COC group, and vibration bands by asymmetric stretching at 1240, 1110, 1165, 960, 732 and 450 cm^{-1} for the COC group have the same behavior of decreasing in intensity, showing the decomposition of PCL according whit infrared spectra of the all composites treated Fig. 8 in part (a)–(d). Fig. 8 shows a decomposition index that relates the bands to 1720 and 1165 cm^{-1} for C═O and COC group vibrations, this relationship confirms the decomposition of the PCL polymer when subjected to the biological assays. Fig. 8 also show in the FT-IR spectra of the composites in the viability test, characteristic absorption band at 1660 cm^{-1} for collagen attributed for amide group C═O. In Fig. 8-f shows an index for the formation of the collagen with time relating the band at 1660 cm^{-1} with the band 1720 cm^{-1} for amide and carbonyl group for collagen and PCL, where it is clearly seen that the collagen is formed with the exposure to the cellular assays, and that it increases with time. Comparing the spectrum of composites fibers treated, the addition of cell resulted in the formation of amide bands for collagen, IR are according with SEM results, the intensity of the amide band increased, indicated certain degree of interaction between the composites and collagen.

4. Conclusions

Four different membrane composites were made by synthesis of crystalline hydroxyapatite and alpha-alumina and the electrospinning method (PCL, PCL-HA, PCL-α-Al2O3, and PCL-HA-α-Al_2O_3), All composites do not show toxicity by the MTT assay, and the compound with greater proliferation at 72 h is the PCL-HA-α-Al_2O_3 membrane. The PCL composite after cell contact shows greater mineralization, followed by the PCL-HA and PCL-α-Al2O3 composites. The compound PCL-HA-α-Al_2O_3 not only allows cell adhesion and proliferation, but also allows mineralization and the formation of collagen fibers. The SEM and FT-IR analyses indicated that chemical interaction between the composite and cell to form collagen.

Data availability

The data used to support the findings of this study are available from the corresponding author upon request.

Funding

This research no received external funding.

Declaration of competing interest

The authors declare that there are no conflicts of interest regarding the publication of this paper.

The authors declare no conflict of interest.

CRediT authorship contribution statement

Ana Karen Monrreal-Rodríguez: Investigation, Formal analysis. **Jesús Alberto Garibay-Alvarado:** Investigation, Formal analysis, Writing - original draft. **Claudia Lucía Vargas-Requena:** Methodology, Resources, Formal analysis. **Simón Yobanny Reyes-López:** Conceptualization, Resources, Methodology, Writing - review & editing, Funding acquisition.

Acknowledgments

Thanks to PRODEP, Universidad Autónoma de Ciudad Juárez and CONACYT for supporting this investigation.

References

[1] M. Mucalo (Ed.), Hydroxyapatite (HAp) for Biomedical Applications, Elsevier, 2015.
[2] H. Wang, Y. Li, Y. Zuo, J. Li, S. Ma, L. Cheng, Biocompatibility and osteogenesis of biomimetic nano-hydroxyapatite/polyamide composite scaffolds for bone tissue engineering, Biomaterials 28 (22) (2007) 3338–3348.
[3] H.W. Kim, J.C. Knowles, H.E. Kim, Hydroxyapatite/poly (ε-caprolactone) composite coatings on hydroxyapatite porous bone scaffold for drug delivery, Biomaterials 25 (7–8) (2004) 1279–1287.
[4] I. Sopyan, A. Fadli, M. Mel, Porous alumina–hydroxyapatite composites through protein foaming–consolidation method, J. Mech. Behav. Biomed. 8 (2012) 86–98.
[5] J.M. Cordell, M.L. Vogl, A.J.W. Johnson, The influence of micropore size on the mechanical properties of bulk hydroxyapatite and hydroxyapatite scaffolds, J. Mech. Behav. Biomed. 2 (5) (2009) 560–570.
[6] D. Cohn, A.H. Salomon, Designing biodegradable multiblock PCL/PLA thermoplastic elastomers, Biomaterials 26 (15) (2005) 2297–2305.
[7] I.K. Kwon, S. Kidoaki, T. Matsuda, Electrospun nano-to microfiber fabrics made of biodegradable copolyesters: structural characteristics, mechanical properties and cell adhesion potential, Biomaterials 26 (18) (2005) 3929–3939.
[8] K. Rezwan, Q.Z. Chen, J.J. Blaker, A.R. Boccaccini, Biodegradable and bioactive porous polymer/inorganic composite scaffolds for bone tissue engineering, Biomaterials 27 (18) (2006) 3413–3431.
[9] M.A. Malik, D.A. Puleo, R. Bizios, R.H. Doremus, Osteoblasts on hydroxyapatite, alumina and bone surfaces in vitro; morphology during the first 2 h of attachment, Biomaterials 13 (2) (1992) 123–128.
[10] S.A. Park, S.H. Lee, W.D. Kim, Fabrication of porous polycaprolactone/hydroxyapatite (PCL/HA) blend scaffolds using a 3D plotting system for bone tissue engineering, Biproc. Biosyst. Eng. 34 (4) (2011) 505–513.
[11] J.H. Roque-Ruiz, S.Y. Reyes-López, Synthesis of α-Al2O3 nanopowders at low temperature from aluminum formate by combustion process, J. Mater. Sci. Eng. 6 (305) (2016) 2169–2222.
[12] T.H. Tran, H.T. Nguyen, T.T. Pham, J.Y. Choi, H.G. Choi, C.S. Yong, J.O. Kim, Development of a graphene oxide nanocarrier for dual-drug chemo-phototherapy to overcome drug resistance in cancer, ACS Appl. Mater. Interfaces 7 (51) (2015) 28647–28655.
[13] Z. Gan, T.F. Jim, M. Li, Z. Yuer, S. Wang, C. Wu, Enzymatic biodegradation of poly (ethylene oxide-b-ε-caprolactone) diblock copolymer and its potential biomedical applications, Macromolecules 32 (3) (1999) 590–594.
[14] M.E. Londoño, A. Echavarría, F. De La Calle, Características cristaloquímicas de la hidroxiapatita sintética tratada a diferentes temperaturas, Rev. EIA (5) (2006) 109–118.
[15] H. Yoshimoto, Y.M. Shin, H. Terai, J.P. Vacanti, A biodegradable nanofiber scaffold by electrospinning and its potential for bone tissue engineering, Biomaterials 24 (12) (2003) 2077–2082.
[16] M.D.L.L.O. Herrera, J.W.O. Castro, Prevalência de nódulos pulpares, Rev. Adm. 58 (4) (2001) 130–137.

[17] S. Kitamura, H. Ohgushi, M. Hirose, H. Funaoka, Y. Takakura, H. Ito, Osteogenic differentiation of human bone marrow-derived mesenchymal cells cultured on alumina ceramics, Artif. Organs 28 (1) (2004) 72–82.
[18] M. Balcerzak, E. Hamade, L. Zhang, S. Pikula, G. Azzar, J. Radisson, R. Buchet, The roles of annexins and alkaline phosphatase in mineralization process, Acta Biochim. Pol. 50 (4) (2003) 1019–1038.
[19] M.G. Donoso, M.L. González-Martín, A.M. Gallardo Moreno, A.M. Vilas, J.M. Bruque, J.L. González-Carrasco, Bioadhesión sobre Alúmina. Propiedades superficiales, 2008.
[20] J. López-Esparza, L.F. Espinosa-Cristóbal, A. Donohue-Cornejo, S.Y. Reyes-López, Antimicrobial activity of silver nanoparticles in polycaprolactone nanofibers against gram-positive and gram-negative bacteria, Ind. Eng. Chem. Res. 55 (2016) 12532–12538.
[21] S.Y. Reyes-López, R.S. Acuña, R. López-Juárez, J.S. Rodríguez, Analysis of the phase transformation of aluminum formate Al(O2CH)3 to α-alumina by Raman and infrared spectroscopy, J. Ceram. Process. Res. 14 (2013) 627–631.
[22] E. Pazos-Ortiz, J.H. Roque-Ruiz, E.A. Hinojos-Márquez, et al., Dose-dependent antimicrobial activity of silver nanoparticles on polycaprolactone fibers against Gram-positive and Gramnegative bacteria, J. Nanomater. 2017 (2017).